Keywords: Large Two-Stroke Engine, Ammonia, Methanol, Combustion, IC Engine, Experimental, Optical Investigation, Simulation

Experimental investigations and simulation validation regarding future fuel combustion systems of low-speed two-stroke engines using WinGD's spray and combustion chamber

Dr. Beat von Rotz, Pascal Süess, Martin Bohnenblust, Dr. Christophe Barro, Dr. Omar Seddik, Juan Reina Martinez, Dr. Andrea Schirru, Dr. Andreas Schmid, Dr. German Weisser

WinGD

https://doi.org/10.18453/rosdok_id00004634

Abstract

In pursuit of the International Maritime Organization's (IMO) ambitious targets for substantial reductions in the carbon intensity and overall greenhouse gas emissions of the shipping industry, a rigorous shift from conventional fossil fuels to alternative, sustainable options are imperative. Among these alternatives, methanol and ammonia have been identified as promising candidates, offering economically viable pathways for decarbonization due to their potential for CO_2-neutral production. Recognizing their significance, WinGD is expanding its product portfolio to include engine technology tailored for ammonia and methanol applications. A prerequisite for a deliberate technology development for future fuel combustion systems is the fundamental understanding of the in-cylinder processes which is established through various experimental studies and numerical investigations.

WinGD's spray and combustion chamber (SCC) is a unique experimental test facility to carry out investigations regarding the injection behaviour and spray/fuel admission characteristics as well as ignition/combustion behaviour and subsequent emission formation at engine-relevant conditions for low-speed two-stroke combustion systems. Optical accessibility allows the application of various (laser-) optical and advanced measurement techniques to examine the in-cylinder processes and their underlying phenomena.

The SCC is equipped to handle the injection and combustion of a wide range of fuels and their combinations. Dedicated fuel conditioning and supply systems have been designed and installed allowing for various operating principles and enabling investigations with a broad variety of fuels, such as standard (distillate and residual) fuel oils as well as alternative liquid/gaseous fuel types especially including alcoholic fuels (e. g. methanol) and ammonia. When operating with such hazardous substances, appropriate safety concepts need to be in place and installations of additional safety measures such as gas detection and ventilation systems are required.

Exemplary results from the high-pressure injection of methanol and ammonia, showcasing the diesel pilot-ignited combustion process under realistic engine conditions with full-scale hardware,

demonstrate the fundamental investigations and studies contributing to a reference database for validating and calibrating WinGD's simulation toolbox. In this respect, the experimentally obtained data from the SCC regarding combustion characteristics and emissions is compared to numerical results derived from 0/1-D models and/or 3-D CFD simulations.

The contribution shall summarize WinGD's dedicated approach for the future fuel combustion system technology development incorporating the pioneering research at engine-like conditions and size from the spray combustion chamber and its utilization for the calibration/validation of numerical models and simulations. The methodology enables a high degree of confidence before engine concepts are implemented at full engine scale for testing and allows well-founded statements regarding the anticipated engine performance.

1. Introduction

The International Maritime Organization (IMO) has set ambitious targets for reducing carbon intensity and greenhouse gas emissions in the shipping industry, necessitating a significant transition from traditional fossil fuels to sustainable alternatives. Methanol and ammonia have emerged as promising options for decarbonization, offering economically viable pathways due to their potential for CO_2-neutral production [1].

The IMO's 2023 revised GHG Strategy includes a reduction of the total annual GHG emissions from international shipping by at least 20%, striving for 30%, by 2030 compared to 2008 levels. Furthermore, the strategy aims for net-zero GHG emissions from international shipping by or around 2050. These targets demand for major technological advancements and adoption of alternative fuels in the maritime sector [2].

WinGD's existing dual-fuel and diesel engine product portfolio already offers the potential for a significant reduction of GHG emissions by being fully capable of using drop-in fuels such as liquid biofuel types and methane from either biogenic sources or synthesis. But such drop-in fuel types will not be available in sufficiently large amounts to cope with the demands of international shipping.

The transition to alternative fuels like methanol and ammonia aligns with the IMO's goal of increasing the uptake of zero or near-zero GHG emission technologies, fuels, and energy sources. The strategy aims for these alternatives to represent at least 5%, endeavouring for 10% of the energy used by international shipping by 2030. This shift is crucial for achieving the long-term objectives of decarbonizing the shipping industry and contributing to global climate change mitigation efforts.

The importance of alternative fuels has been recognized and engine manufacturers are expanding their product portfolios to include technology specifically designed for ammonia and methanol applications. Well noting that WinGD committed itself towards decarbonization and implemented dedicated strategic actions to considerably invest into alternative fuel technologies years before IMO's revised GHG reduction strategy was adopted [3-4].

This did not only involve the commitment to put substantive efforts into such activities but also feature a considerable extension of workforce as well as infrastructure, especially in our global testing & validation facilities [5], for the validation of the technologies under development.

1.1. WinGD's Future Fuel Technology Development Approach

The rapid and successful development of novel technologies to apply methanol and ammonia with a large two-stroke marine diesel engine combustion system requests for fundamental understanding of the phenomena regarding fuel injection and spray formation, ignition behaviour and combustion characteristics as well as emission formation. WinGD's dedicated spray combustion chamber (SCC) is allowing detailed investigations of key components and parameters already in the early stages of the technology development process.

The project timeline for the methanol and ammonia engine development program was exceptionally tough, with initial deliveries scheduled for early 2025. This ambitious aim drastically reduced the window for traditional testing and concept validation. To address this challenge, the team implemented a robust frontloading strategy, heavily emphasizing on numerical development tools which have been validated and calibrated by experimental data from SCC investigations (see Figure 1). This approach enabled rapid iteration and verification of design concepts, allowing the project to maintain its

ambitious timeline while still ensuring thorough evaluation of all critical components. By leveraging advanced simulation technologies, the team aimed to mitigate the risks associated with the tight development plan and meet the unprecedented engine delivery targets.

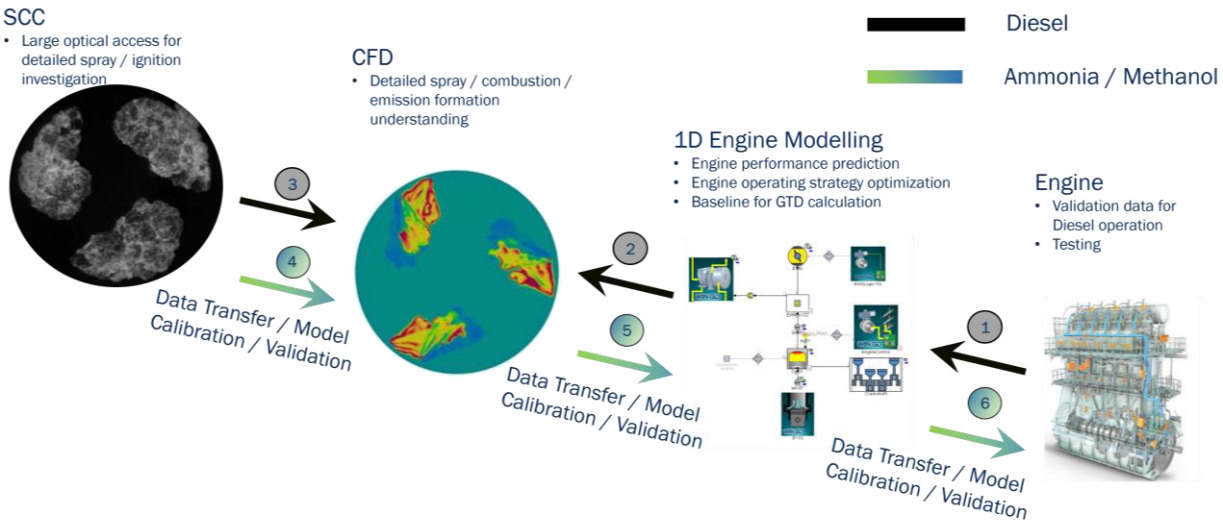

Figure 1: Illustration of WinGD's methanol and ammonia engine development approach highlighting the main process steps (1-6).

The simulation toolbox applied for investigating the combustion system behaviour and ultimately predicting the key performance parameters consist of a 1-D engine model using GT-POWER and 3-D Computational Fluid Dynamics (CFD) simulation by means of CONVERGE CFD, in combination with a variety of enhancements and specifically tailored sub-models such as chemical reaction kinetics.

Besides data from various lab engines, also measurement sets acquired for the complete portfolio in the course of prototype tests as well as series engine confirmation trials have been incorporated into the simulation tool development (Figure 1: step 1). The resulting model was further validated by applying it to the specific conditions and domain of the SCC. This step ensured accurate predictions of initial conditions for spray, ignition, combustion, and emission simulation results using CFD in diesel operations. Additionally, it confirmed the transferability of combustion characteristics obtained through CFD to 1-D engine simulations. (Figure 1: step 2).

The subsequent validation effort then consisted in the assessment of the CFD results against the experimental data obtained on the SCC for a large range of key parameter variations, first for operation on conventional diesel type fuels, then followed by a similar exercise for the methanol/ammonia combustion (Figure 1: step 3/4). This requires an iterative process between experiment and simulation in order to make sure that the modelling approaches used for all relevant processes properly reflect the effects and characteristics inside the SCC and its subsystems.

The successful validation/calibration of the underlying models of the CFD simulation with the obtained data from the SCC paved the way for the next steps along the designated development approach. This phase involved creating a parametric model of the combustion system with methanol/ammonia serving as a primary fuel and diesel as pilot source (Figure 1: step 5). To validate this 1-D model, simulations with the SCC domain were utilized and subsequently, the resulting tool was employed to forecast engine performance parameters for the laboratory test engine platforms where the X-DF-A as well as X-DF-M combustion concepts are tested and validated (Figure 1: step 6).

Furthermore, the agreeing results gave high confidence in applying the developed models to design the combustion system for the first production engines along the announced portfolio program. This proactive approach allows for concurrent development and refinement, optimizing the timeline from concept to production.

2. Experimental Setup

2.1. Spray Combustion Chamber SCC

This unique experimental research test facility enables comprehensive investigations into injection behavior, spray/fuel admission characteristics, ignition/combustion dynamics, and subsequent emission formation. The versatile setup allows for experiments under engine-like conditions, with peak firing pressures up to 20 MPa, relevant for large marine engine combustion systems representative of smaller-size two-stroke and larger four-stroke engine configurations.

To achieve the high pressure and temperature conditions of the gas prior to fuel injection, two pressurized vessels are filled with air or a desired gas mixture (e.g. non-reactive, EGR). By precisely controlling the filling time of the two main valves, pressurized gas from the pressure vessels enters the regenerator and is heated to a temperature comparable to that after the compression stroke. A specially designed intake system between the regenerator and SCC reproduces the strong gas swirl motion within the combustion chamber, mimicking conditions in real engines from WinGD [6-10].

The fuel injection system at the SCC has been further refined and developed with dedicated conditioning and supply systems installed for various fuels [5]. As illustrated in Figure 2, the SCC is capable of investigating high-pressure injected fuels (e.g. methanol, ammonia). To ignite these future fuels, an upstream injector delivers a small amount of diesel to initiate and enhance the subsequent combustion of the downstream main injection.

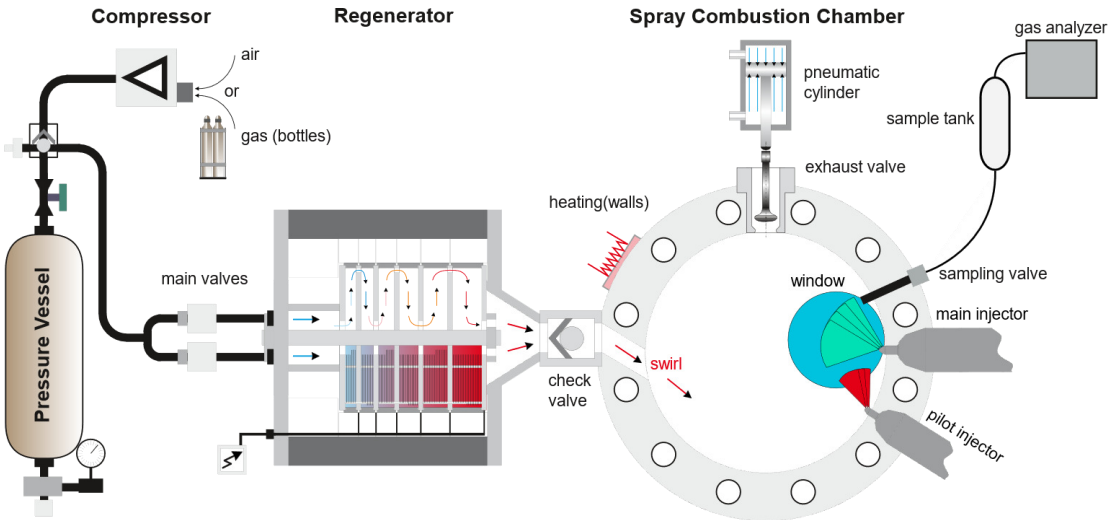

Figure 2: Schematic of the spray and combustion chamber test rig with the associated devices for charge conditioning (pressure, temperature) as well as piloted high-pressure fuel injection setup and emission sampling system.

A specially designed exhaust gas sampling system enables the precise collection of exhaust gas during or after combustion, which can then be analysed using advanced emission measurement devices to accurately quantify the concentrations of individual chemical species present in the exhaust. This system allows for real-time sampling and high-precision collection methods, ensuring the integrity of the

samples throughout the analysis process. With the aforementioned fuels, formaldehyde, nitrous oxide, and ammonia are of particular interest due to their significant environmental impact and role as indicators of combustion efficiency. The ability to accurately measure these compounds provides valuable insights for emissions research and the development of cleaner combustion technologies.

Optical accessibility is provided through sapphire windows with diameters up to 180 mm, offering exceptional clarity and durability for visual observations. The combustion chamber is equipped with eccentric window holders and fixed window positions in a rotatable cover, enabling comprehensive visual access to any location within the chamber.

2.2. Optical Diagnostics and Data analysis

The optical setup used for the experiments on the SCC consists of four high-speed CMOS cameras (3x Photron NOVA S16, 1x Photron HSS6) together with a lens-coupled image intensifier (LaVision IRO) and a pulsed diode laser as a light source (Cavitar Cavilux).

The schematics of the optical setup used for various injection and combustion studies are depicted in Figure 3. Camera 1 captures the Mie-scattering from the fuel spray, which is illuminated by an expanded diode laser beam. A tele-zoom lens attached to the camera provides magnification, enhancing the spatial resolution and allowing for detailed visualization of the spray's structure, atomization, and evaporation. Cameras 2 and 3 cover an identical field of view, but the light is separated by a dichroic mirror. The visible part is transmitted and directed by a second mirror towards Camera 2, which acquires colour images of the flame luminosity. These images enable detailed study of flame propagation and characteristics. The light with a wavelength below 400 nm is reflected by the aforementioned dichroic mirror and used for OH*-chemiluminescence imaging. For this purpose, Camera 3 is equipped with a band-pass filter at 310 nm, an UV-lens, and a lens-coupled image intensifier. This optical technique enables the detection of spatial initiation of ignition and combustion in the intensified, non-visible wavelength range. Moreover, a newly developed ultra-wide angle high-speed imaging setup (camera 4) is implemented to record not only the flame characteristics near the nozzle but also its propagation through the entire combustion chamber. This setup provides unique and unprecedented insights into the combustion system of a large two-stroke Diesel engine.

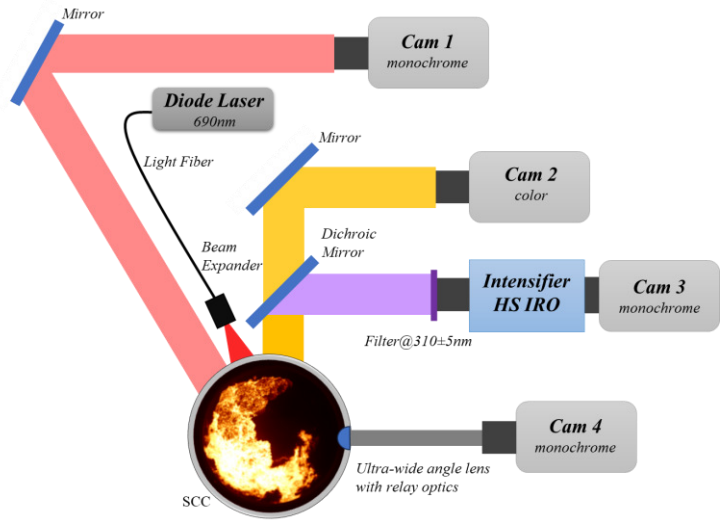

Figure 3: Schematic of optical measurement setup applied at the SCC with simultaneous Mie-scattering, OH-chemiluminescence and flame-luminosity in both, near nozzle and ultra-wide angle view.*

The heat release rate (HRR) is calculated via the pressure and temperature trace measured in the SCC. In order to consider the heat losses for the rate of heat release, which are additionally increased due to the high swirl velocities present during filling and combustion, the derivative of the pressure signal before and after the combustion is analysed. Hence, the heat losses before start of combustion as well as after its ending are calculated and corrected, accordingly. As a simplification, the heat losses during the combustion are linearly approximated.

3. Combustion Visualization and Characteristics

The SCC played a pivotal role in developing WinGD's methanol and ammonia engines by facilitating the first-ever combustion of both fuels in a large two-stroke combustion system environment. Its unique capability to optically study ignition and combustion processes at these length scales provided highly valuable reference data for CFD validation, complementing conventional engine data such as heat release calculated from in-cylinder pressure as well as emission characteristics provided by the advanced exhaust gas sampling system. Example data of a single pilot/main injection configuration and detailed analyses will be explained in the following sections.

3.1. Methanol

The methanol combustion characteristics are described via an exemplary experiment conducted at a typical engine operating condition of 50% load with pressure and temperature before the injection being 116 bar and 860 K, respectively. For this experiment, the fuel flexibility of the SCC [5] allowed a rapid exploration of a new fuel as without changing the standard (diesel) injector positions, one injector could be converted to methanol operation, while its upstream counterpart was operated with diesel for piloting. For subsequent measurements, the position of the pilot injector was brought closer to an engine-like setup with a shorter distance between the two injectors.

The timing of the pilot injector was set to ensure the pilot flame reaches the methanol spray way before conditions allowed a self-ignition of methanol. In the first image in Figure 4 at 5.4 ms after start of pilot injection, the pilot flame is approaching the position of the main injector, which just has started injecting liquid methanol. The second image (at 7.4 ms) captures the moment where the diesel pilot flame first contacts the methanol spray. An instant ignition of the methanol fuel occurs at this time and location. Subsequent images (at 8.4 and 11.4 ms) show the propagation of the methanol flame throughout the spray, eventually reaching a stable lift-off length from the injector.

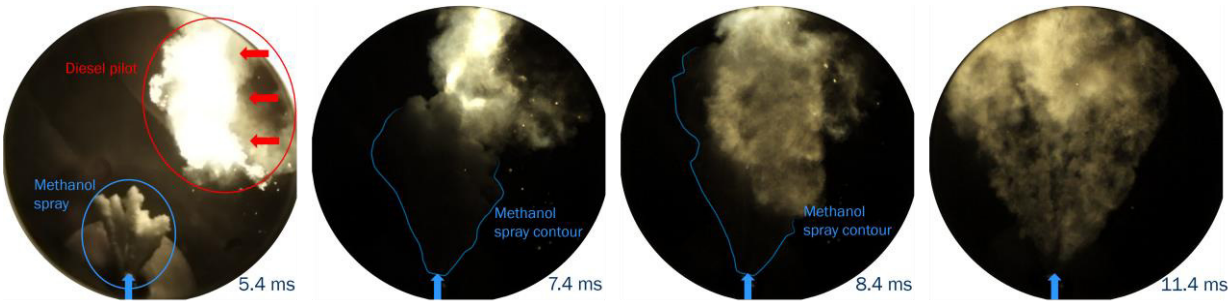

Figure 4: Flame luminosity image sequence showing the diesel piloted (red) high-pressure methanol (blue) injection and combustion process (near main injector view).

Besides the high-speed image acquisition, also relevant pressures and temperatures are recorded in the combustion chamber. From these signals the rate of heat release can be derived, which is a key

parameter for the characterization of combustion phenomena and provides valuable insights into the combustion process. Figure 5 is showing the HRR and the corresponding cumulative heat release in relation to the aforementioned experiment.

For this measurement configuration and pilot/main timing, the added heat from the pilot combustion as well as the exact ignition time can be clearly recognized in the graph. Following the methanol ignition, the initial peak is attributed to the premixed part of the combustion which occurs until a stable flame is established. After this premixed peak, the combustion is followed by a transition to fuel-air mixing controlled phase, resulting in a distinctive diesel-like heat release rate shape.

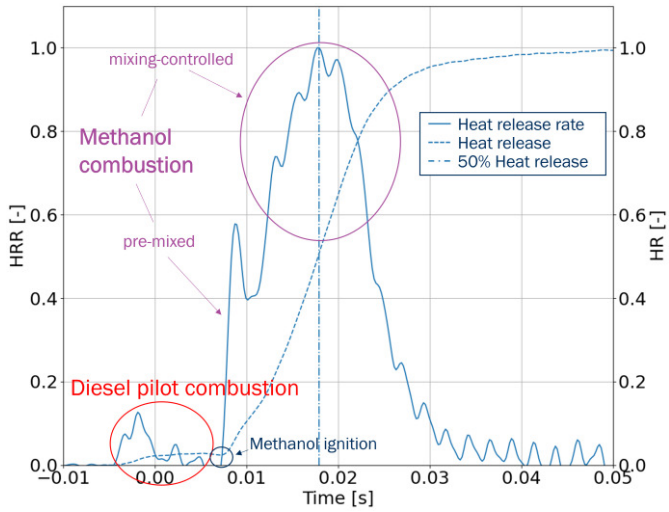

Figure 5: Heat release characteristics of a diesel pilot-ignited high-pressure injected methanol combustion.

During these comprehensive investigations of methanol combustion, a large variety of different conditions including variations in injection pressure, gas temperature/pressure, pilot and main energising time and timing, atomizer execution, pilot-to-main setup and main injector temperature were examined. Under each condition the before mentioned signals as well as the derived heat release rate were explored, exhaust emissions and high-speed images were analysed. The resulting dataset served as basis for validating and calibrating our 0/1-D and 3-D simulation models, which are described in subsequent sections.

3.2. Ammonia

Hereafter, the experiments from the first-ever ammonia combustion in a large two-stroke engine combustion system environment are presented. The optical data was acquired using an ultra-wide-angle camera inserted into center of the combustion chamber cover, enabling comprehensive investigations of the pilot ignition/combustion, and subsequent ignition of the liquid-injected, atomized, and evaporated ammonia throughout the entire combustion chamber. As with the methanol case, this experiment was conducted at the same operating condition with pressure and temperature before the injection being 116 bar and 860 K, respectively.

In Figure 6, the first image (at 5 ms after start of main injector energising) captures the diesel pilot flame directed towards the main injection. The intense luminosity of the soot from the diesel flame leads to a very high exposure signal of the pilot spray in the recordings but also illuminates the liquid ammonia injection. In order to visualize the various characteristics of the diesel piloted high-pressure ammonia combustion, the images have been individually intensity corrected. The not yet fully ignited

ammonia spray can be clearly distinguished in the second image (at 10 ms) as a dark cloud within the bright diesel pilot flame. As the combustion of the ammonia proceeds, the turbulences increase, causing the pilot flame to become fragmented and dimming the overall exposure (image 3 at 15 ms). The heavily intensified images 4-6 (20 - 30 ms) reveal the propagation of the ammonia flame through the combustion chamber as the overall illumination by the remaining diesel pilot rapidly decreases.

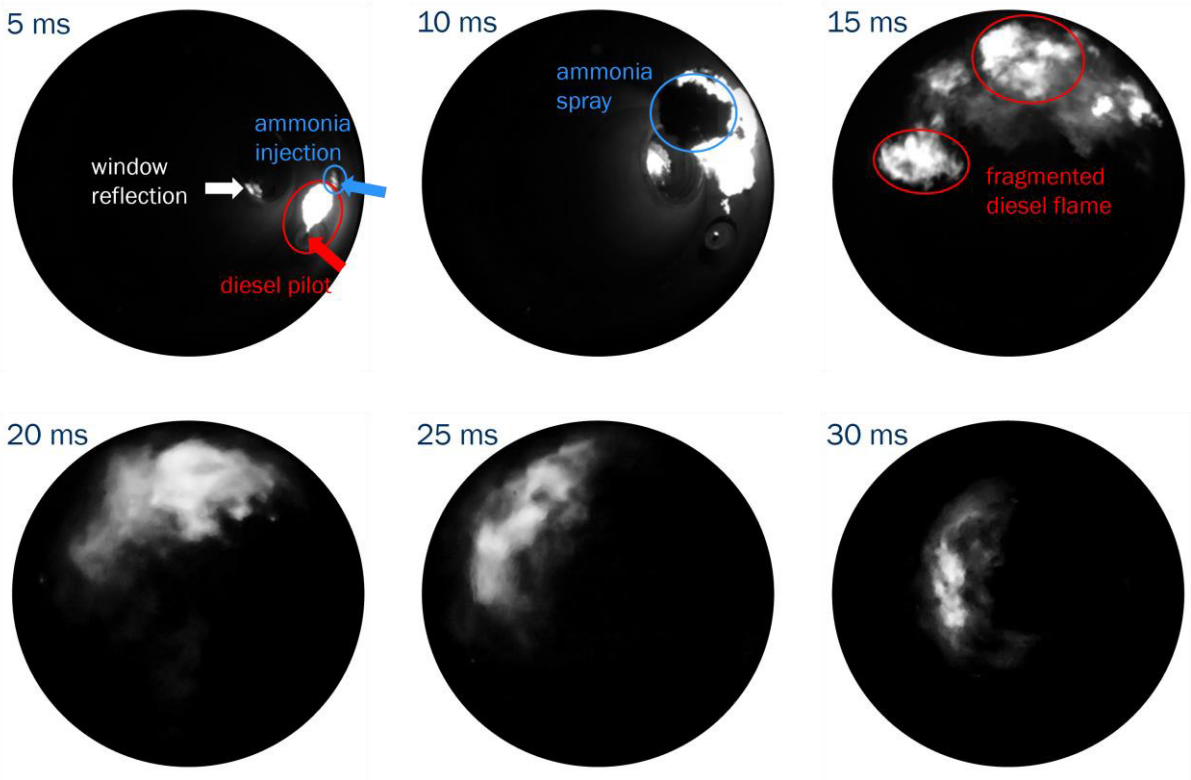

Figure 6: Flame luminosity image sequence of a diesel piloted (red) ammonia (blue) ignition and combustion process between 5 ms and 30 ms after start of main injector energizing (ultra wide-angle view).

Figure 7 shows the derived rate of heat release for the ammonia combustion. With the pilot/main injector setup and timing for this experiment, the diesel pilot combustion is directly followed by the ammonia combustion and thus no distinct separation in the HRR plot can be recognized. The HRR for a piloted ammonia combustion related to a large two-stroke engine system can be divided into two distinct phases: The first phase, starting with the ignition of the ammonia by the diesel pilot flame, is mainly governed by the premixed combustion of the injected ammonia. After a short transition phase where the HRR decreases significantly, the second phase of the ammonia combustion can be observed. At this stage the HRR is generally governed by the mixing rate but also significantly superimposed with (comparably slow) chemical reaction rate of ammonia. As the gas pressure and temperature are rising during the combustion, the chemical reaction rate accelerates, leading to a steady increase in HRR until fuel availability decreases (the ammonia injection has stopped slightly before the peak in the second phase, ca. at 40 ms) and the HRR slowly drops to zero.

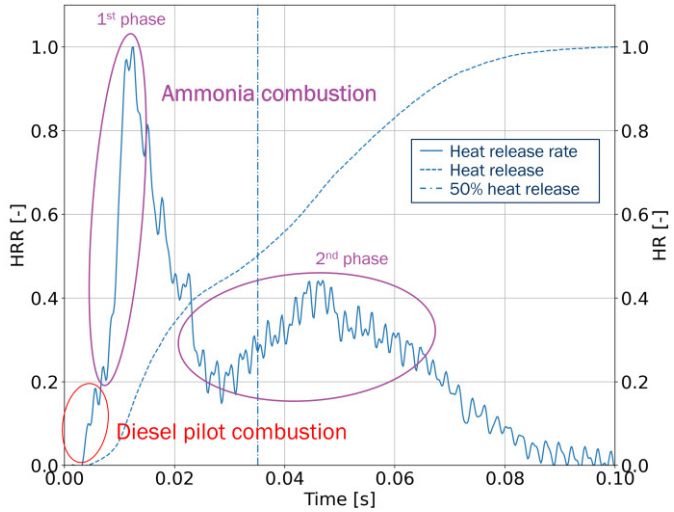

Figure 7: Heat release characteristics of a diesel pilot-ignited high-pressure injected ammonia combustion.

In a similar manner, to gather a vast data set for the validation and calibration of our simulation models, different variations were studied, such as injection pressure, compression pressure and temperature, energising time, pilot timing, main injector temperature, main injector configuration, swirl and a variety of different piloting strategies.

In this contribution for each fuel (methanol and ammonia) only the flame luminosity high-speed visualizations are exemplarily shown (colour camera and ultra-wide angle camera setup). It is worth noting that for the vast majority of experiments conducted under this experimental campaign, all available imaging systems were used for both fuels. Furthermore, the presented results show a single pilot/main in order to focus on the validation and calibration of the main phenomena such as the injection and spray formation as well as combustion model adjustments where these data already generate a highly valuable reference data set. Subsequently, experiments with multiple single pilot/main injector setups have been performed and are under evaluation.

4. Simulation Toolbox: Validation and Calibration

CFD simulations are invaluable tools for both design-oriented and research-oriented activities, as they enable the exploration of new designs - such as injectors with different features or changes in engine geometry - without the high costs and long lead times associated with manufacturing new parts or operating the engine. These simulations can quickly deliver results and provide detailed local information about what occurs inside the cylinder with very fine resolution. This capability is crucial for our application, as the operating costs for testing a two-stroke engine are exceptionally high and many tests can be efficiently conducted in a virtual environment using CFD. However, to ensure the accuracy of CFD models, they must be validated against real-world data by comparing results from simulations with experimental data. In our case, we compare performance parameters such as pressure, apparent heat release rate (AHRR) and emissions, as well as the morphology of the flame. These comparisons are challenging and expensive to perform directly on the engine, particularly in the early stages of development where design and manufacturing of most of the components is still not consolidated. Furthermore, safety precautions can be considered within a much smaller framework, and it results in an environmental benefit when comparing with full size engine testing. Therefore, the initial step in validating our models occurs within the SCC, where the geometrical characteristics and

ambient conditions (pressure, temperature and swirl) closely resemble those of the engine. This controlled setup allows us to compare simulations and experiments while accessing detailed information, such as flame and spray features, that would not be available in engine tests.

For this numerical campaign, 3-D CFD simulations were conducted using CONVERGE, which offers a range of combustion and spray models as well as meshing features specifically designed for simulating internal combustion engines. The combustion process was modelled using the SAGE combustion model [11] which relies on detailed kinetics. The simulations covered both the filling process of the SCC and the combustion phase, using time-varying boundary conditions and initial conditions derived from experiments. This approach ensured an accurate description of the flow field inside the SCC at the start of injection (SOI).

The computational grid employed for the simulations had a base size of 2.5 mm, with local refinements in the regions near the diesel and ammonia/methanol injectors. An adaptive mesh refinement (AMR) technique, based on velocity, temperature, and species gradients, was used to more precisely describe the ignited jet, achieving a minimum mesh size of approximately half the injector nozzle diameter. This mesh resolution is crucial for maintaining contained void fraction values, which are essential for the KH-RT breakup model used in this investigation to accurately predict spray morphology and evaporation. Lastly, turbulence was modelled using the RANS approach with the well-known two-equation k-ε model.

4.1. Methanol Simulation Results

In this section, the main results for the comparison and validation of the CFD model to experimental results for methanol will be presented. In Figure 8, a comparison between the normalized experimental and CFD AHRR is shown for the three energizing times (15, 20 and 25 ms) at 50% load conditions (116 bar and 860 K before start of main injection). The normalization was done on the basis of the maximum experimental HRR. In general, the pilot ignition delay is well captured, with just a slight overprediction by the CFD in comparison to the experiment, and the peaks of the pilot combustion are well matched. Additionally, it can be observed, especially from the CFD AHRR curves, that there is a small premixed portion of the combustion. A small peak can also be seen in the experimental HRR but it is less pronounced as in the simulation curve which partly can be attributed to the signal processing of the experimental raw data of the pressure measurement. The transition from premixed combustion to mixing controlled is slightly slower in the CFD than the AHRR computed from the experiment. However, the overall combustion duration, heat release peak and fall off are in good agreement with the experiment, the last being a critical factor in NO_x formation prediction.

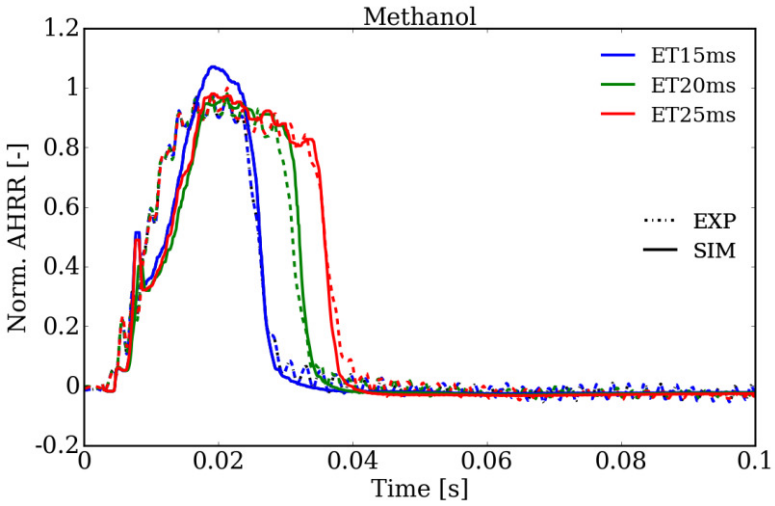

Figure 8: Normalized Apparent Heat Release Rate for methanol combustion at different main injector energising times.

In Figure 9, a comparison of the temporal evolution of the flame is shown at intervals of 5 ms after start of main injector energizing. The top row depicts the CFD results, represented by iso volumes of temperature, while the bottom row shows the experimental images at the same time step, accordingly. The swirl effect of the SCC can also be recognized in the images and generally, the agreement between CFD and experiment in terms of overall shape and location of the tip is very reasonable.

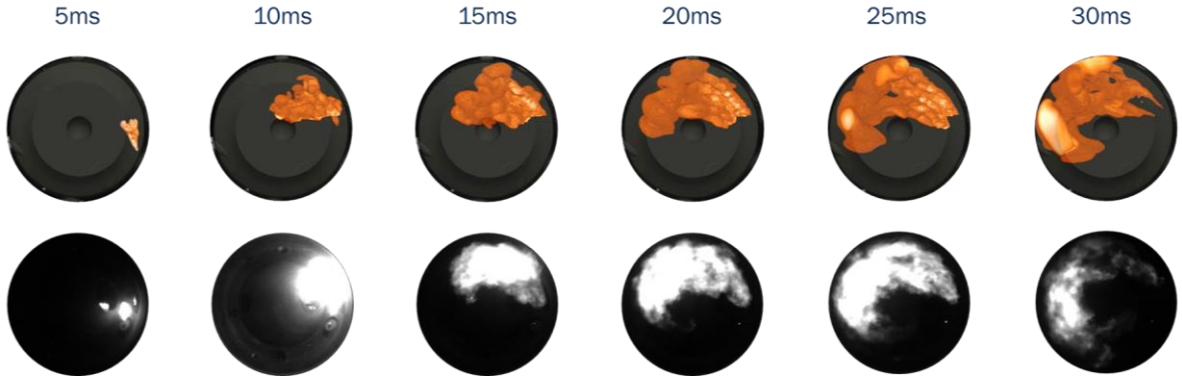

Figure 9: Comparison of the temporal evolution of the methanol flame within the combustion chamber between CFD (top) and experiment (bottom).

Figure 10 presents a bar graph of the NO_x emission comparison between CFD and experiment at the three energising times. An error bar is indicated for the experimental data which was measured as the maximum variation measured for a given condition during multiple instances of the same test. The values are normalized by taking as reference the maximum value from experiments. NO_x of CFD is calculated using an extended Zeldovich mechanism as there is no NO_x path in the used chemical mechanism. Generally, CFD slightly over-predicts NO_x emissions, but the overall trend is well matched as the NO_x increases with longer injection durations.

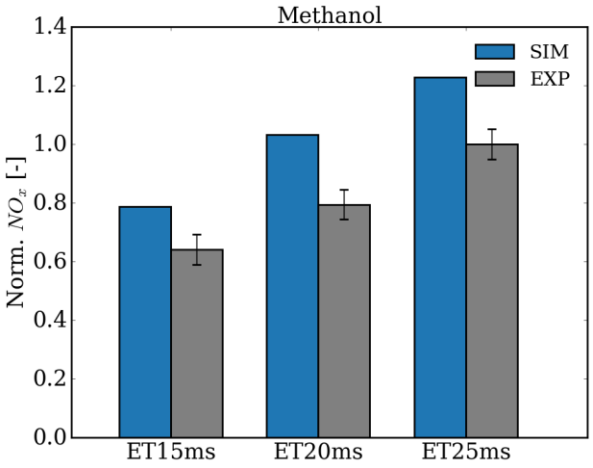

Figure 10: Comparison of normalized NO_x emissions between simulations and experiments at different main injector energising times.

4.2. Ammonia Simulation Results

Figure 11 presents a comparison between the simulated and experimental AHRR curves for an ET variation at 50% load conditions (116 bar and 860 K before start of main injection), with values normalized to the maximum experimental AHRR across all conditions. Qualitatively, the numerical setup successfully reproduces the main characteristics observed in the experiments. The simulations accurately capture ignition delay times for both pilot and main, indicating that the chemical scheme and the interaction between pilot and main injection are well-represented. Additionally, the model accurately identifies the AHRR drop characteristic of conditions with an ET ranging from 30 to 50 ms. This decrease in the AHRR signifies a transition from the first combustion phase, governed by a mostly premixed regime, to a second phase where the prolonged chemical timescales characteristic of ammonia combustion additionally influences the rate at which heat is released. This superimposing phenomenon is due to the significantly longer chemical ignition delay compared to evaporation and mixing times, preventing the ammonia flame from stabilizing under the selected ambient conditions.

The overall combustion duration and the second AHRR peak at the end of injection are also well predicted by the model, demonstrating sensitivity to variations in ET. However, the simulations tend to overestimate the premixed peak, likely due to the underlying assumptions of the combustion model. While the SAGE model provides detailed chemical predictions, it does not fully account for the effects of the turbulence field on the chemical evolution of the combustion. This simplification can lead to a slightly faster ignition of the mixture, resulting in an overestimation of the heat release rate during the premixed phase. Consequently, this overestimation impacts the predicted NO_x emissions, which are generally higher in the simulations, as shown in Figure 12a (values are normalized by taking as reference the maximum value from experiments). Despite this, the model accurately predicts the trend of NO_x emissions variation with energizing time, indicating higher NO_x emissions for longer injections.

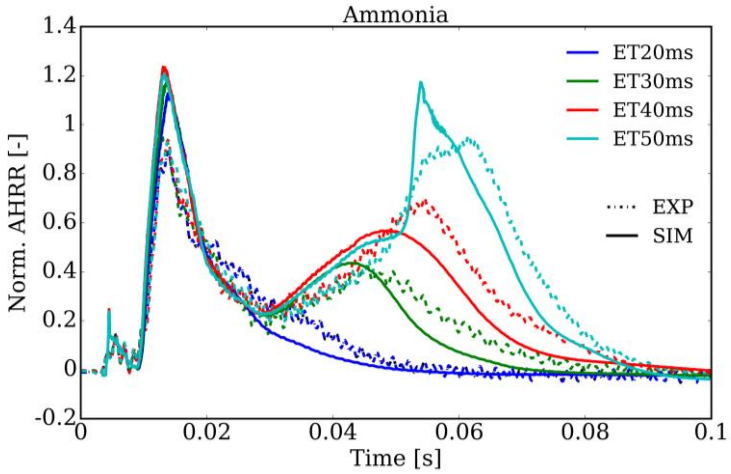

Figure 11: Normalized Apparent Heat Release Rate for ammonia combustions at different main injector energising times.

Figure 12b illustrates that NO_x production occurs in two phases: an initial phase during the premixed combustion event, followed by stabilisation during the transition phase between combustion regimes and a second production phase.

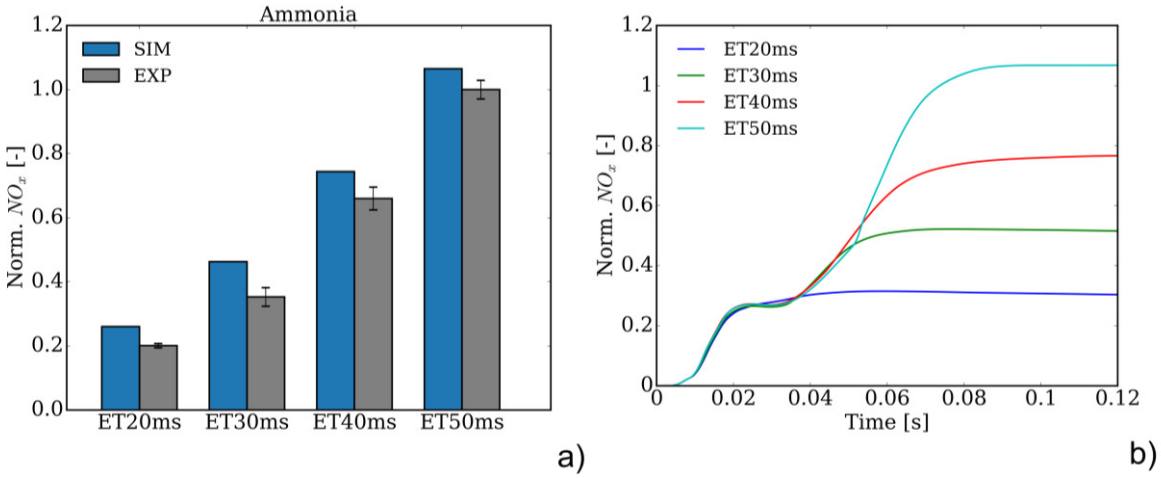

Figure 12: Comparison of normalized NO_x emissions between simulations and experiments at different main injector energising times (b) as well as time-resolved NO_x simulation values (a).

In Figure 13, temperature, NO mass fraction and equivalence ratio are shown on a slice cutting through the main ammonia jet. The ignition of a largely lean ammonia-air mixture is evident, leading to the initial production of NO_x in the ignited region of the ammonia jet. The figure also illustrates the inability of the ammonia flame to stabilize, causing the lift-off length to increase steadily during the combustion process. Consequently, combustion occurs far from the nozzle tip, while, in the vicinity of the injector, a significant amount of ammonia is left to mix with the surrounding air without participating to this stage of the combustion. The process is then largely governed by ammonia's chemical timescales, which control the rate of fuel consumption. As pressure and temperature rise within the SCC, the mixture's reactivity increases, enhancing the fuel's burning rate and causing the second peak shown in Figure 10. Following this peak, the scarcity of ammonia in the SCC leads to a gradual decrease in AHRR until the combustion process is complete.

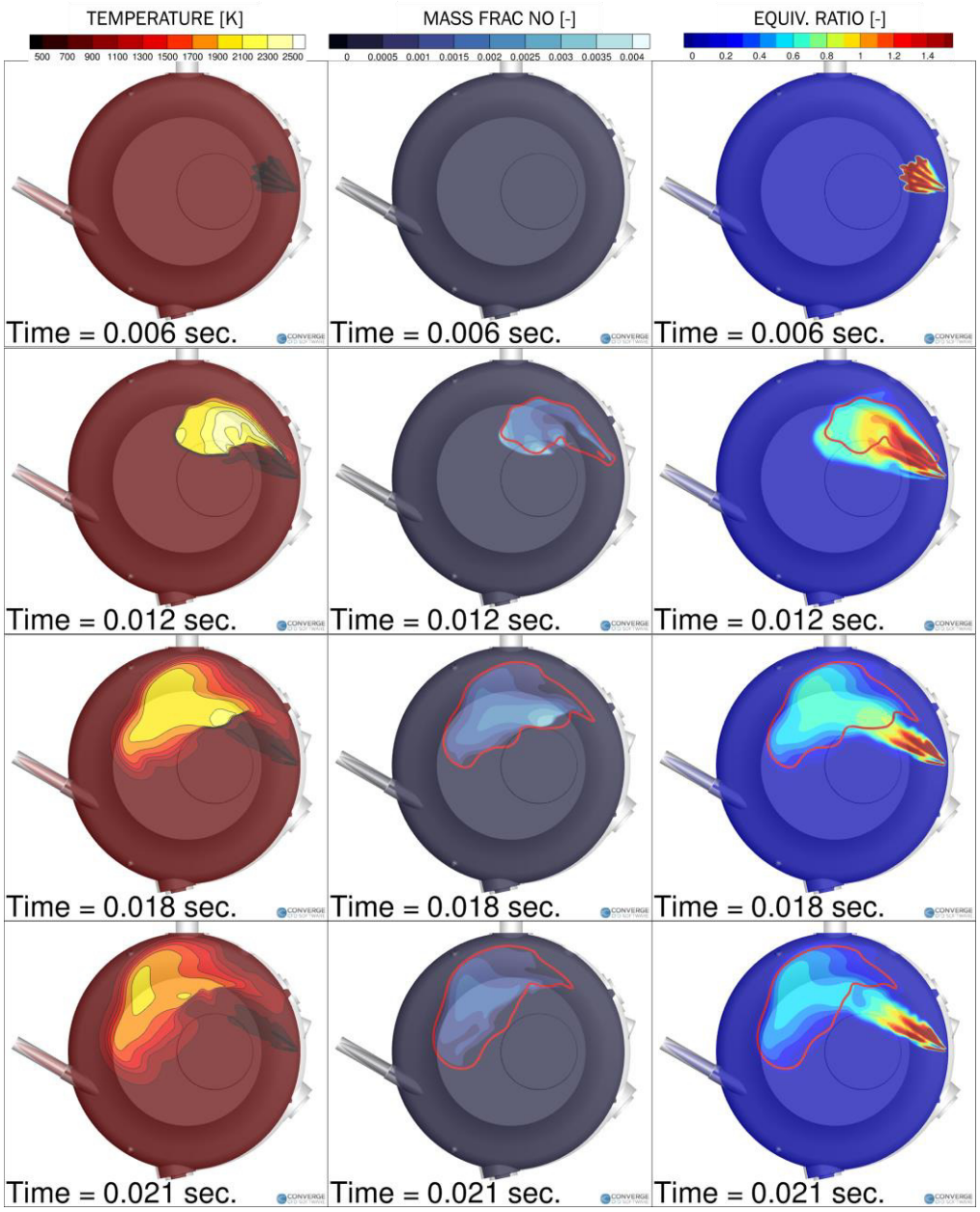

Figure 13: CFD results for ammonia combustion showing temperature (left), NO mass fraction (middle) and equivalence ratio (right) fields. The highlighted red line represents an iso-line of temperature at 1200 K. The condition showed here is that with ET of 30 ms for the main injection.

When discussing ammonia combustion, one significant concern is the production of nitrous oxide (N_2O) emissions. N_2O is a potent greenhouse gas with a global warming potential of 298 times that of CO_2 over a 100-year period [12]. In Figure 14, a comparison between experimental and simulated values of N_2O emissions is presented (values are normalized by taking as reference the maximum value from experiments.). It is observed that the CFD model consistently overestimates the production N_2O compared to experimental data. While this indicates that there is a potential for further improvement in the chemical mechanisms used in the simulation, it also provides a conservative estimate when applied to real engine scenarios. This conservative nature of the CFD model ensures that any predictions made will likely overestimate the actual emissions, providing a safer margin for engine performance considerations.

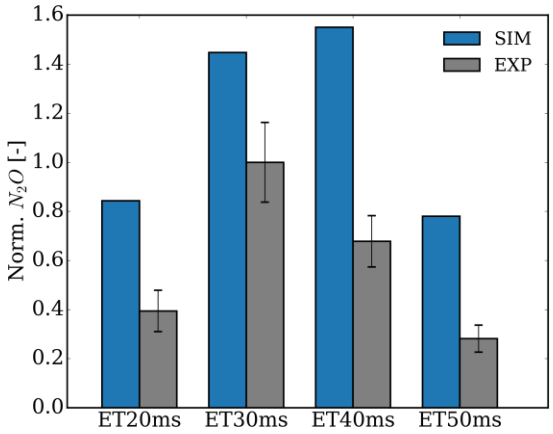

Figure 14: Comparison of normalized N_2O emissions between simulations and experiments at different main injector energising times.

4.3. Methanol 0/1-D Modelling Results

The prediction of engine performance and emissions is a necessity in the development of marine engines, since the number of engines with the exact same configuration is small and engines with new configurations or fuels are potentially sold way before they are built. For this reason, a combustion and emission model methodology has been developed for integration into a one-dimensional engine simulation environment. According to the presented approach in this contribution, the methodology has been adapted for the methanol as well as ammonia combustion system development. Hereafter, the corresponding considerations are exemplarily described for the methanol application.

The CFD investigation showed along with the measurements, that for diesel as well as for methanol, the majority of the fuel is converted in a mixing controlled manner. Therefore, a simplified combustion model has been developed, which was calibrated using the measured heat release rate from the spray combustion chamber. The combustion model describes only the mixing controlled combustion phase. It uses an underlying spray model and nozzle characteristics to estimate the turbulent kinetic energy and dissipation rate from the fuel spray. In addition, the combustion chamber background turbulence level is estimated. The goal of the spray-based combustion model is to reproduce the characteristic mixing rate. The characteristic mixing rate ν_{mix} is defined as follows:

$$\nu_{mix} = \frac{HRR(t)}{Q_{avail}(t)} = \frac{HRR(t)}{\int_0^t \left(\dot{q}_{inj}(t) - HRR(t)\right) dt} \tag{1}$$

This simplified definition of the characteristic mixing rate follows the assumptions that the ignition delay is insignificant in contrast to the injection duration and the evaporation time of the fuel is insignificant in contrast to the mixing of the air and the fuel. The injected energy (blue, diesel), the heat release rate (red) and the according characteristic mixing rate (black) are depicted in Figure 15. The figure shows three operating conditions with a variation in injection duration: a short (dashed), a medium (solid), and a long injection duration (dash-dotted). The mixing rate during injection is increasing due to the increase of pressure during combustion. This effect is particularly strong in the spray combustion chamber due the absence of an expanding volume. The small drop in mixing rate after injection indicates a high background turbulence level, which is originating from the spray combustion chamber filling process.

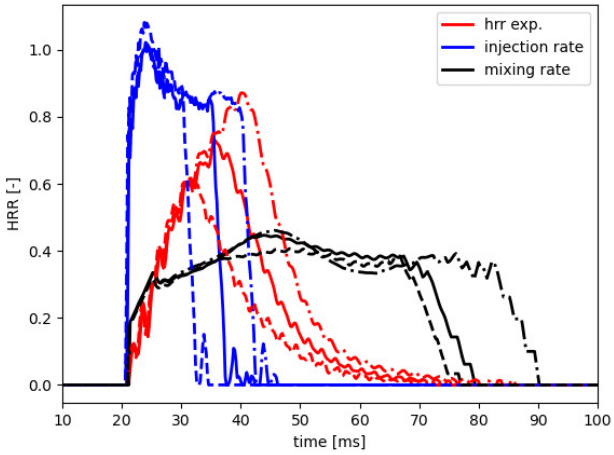

Figure 15: Injected energy rate (blue), heat release rate (red) and mixing rate (black) of three different diesel injection durations (dashed, solid, dash-dotted).

Figure 16 shows the measured versus modelled heat release rates after calibrating the turbulence parameters in the combustion model. The injection and the heat release rate are equally coloured as in the previous figure, the modelled heat release rate is plotted in black. The modelled heat release rate shows a very high accuracy to the measured one.

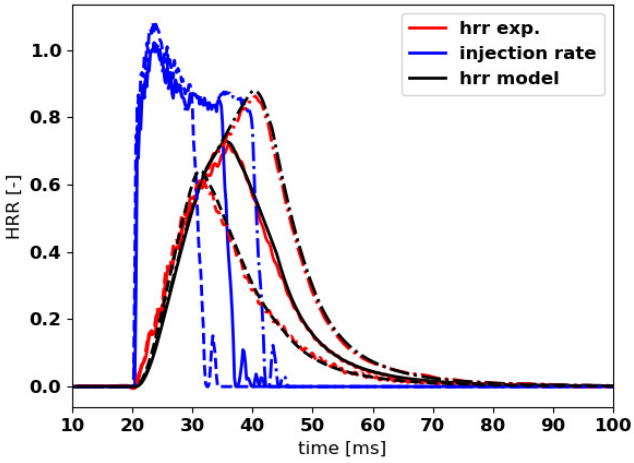

Figure 16: Injected energy rate (blue), measured heat release rate (red) and modelled heat release rate (black) of three different diesel injection durations (dashed, solid, dash-dotted).

The model calibration has been minorly adapted and applied to three different operating conditions using methanol as a fuel (and a small percentage of diesel to support the ignition). Figure 17 shows the injected energy rate (blue, methanol), the measured heat release rate (red) and the modelled heat release rate (black) for three different injection durations (solid, dash-dotted and dashed). In contrast to diesel, methanol shows a significantly reduced lower heating value. In addition, due to the oxygen content of methanol, the stoichiometric air-to-fuel-ratio is lower. As a consequence, the required time to mix to stoichiometry is shorter for similar spray conditions. Consequently, the combustion rate is higher and the heat release rate is closer to the profile of the injection rate. The results show that this type of model is very well capable to reproduce this combustion behaviour.

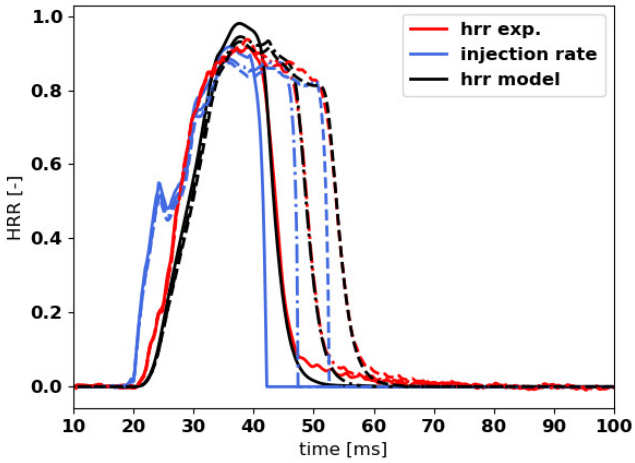

Figure 17: Injected energy rate (blue), measured heat release rate (red) and modelled heat release rate (black) of three different methanol injection durations (dashed, solid, dash-dotted).

This combustion modelling methodology was then transferred to an engine simulation environment, where the combustion model could also be calibrated using inputs from CFD. This setup allowed engine simulations with broad variations in operating conditions at minimum computational costs and experimental effort, which have been used for determining the best selection of injection system layout as a basis for the subsequent optimisation of the associated parameters.

5. Conclusions

The rapid development of methanol and ammonia technologies for large two-stroke marine diesel engines has indeed required a fundamental understanding of fuel injection, spray formation, ignition behaviour, combustion characteristics, and emission formation. WinGD's dedicated spray combustion chamber enables detailed investigations of key components and parameters early in the technology development process. The exemplary visualizations and characteristics of the diesel-piloted high-pressure injected methanol and ammonia combustion provide an insight into the investigations for an in-depth understanding of the underlying phenomena. This is especially important when focusing on the unique behaviour of the onset of combustion by the pilot as well as the subsequent heat release of methanol and, in particular, ammonia.

Generating this highly valuable reference data set enabled the application of a robust frontloading strategy. It includes information on hydraulic injector performance, injection behaviour and spray formation as well as important characteristics of the piloted main ignition and combustion process at various cell conditions and configurations (e.g. pilot/main energizing time and timing, injection pressure, injector temperature and atomizer configurations). Furthermore, the investigations were complemented with essential insights into emission formation and characteristics.

The presented approach heavily emphasizes numerical development tools, validated and calibrated by a comprehensive set of measurements from SCC experiments. For methanol as well as ammonia a selection of CFD simulations is shown, highlighting the validation and calibration procedure to further develop or adjust the sub-models for the spray formation, the combustion model and subsequent emission formation. These detailed investigations revealed the similarities of the methanol combustion process with diesel but even more interesting the peculiarities of a not mainly mixing-controlled combustion phase when operating ammonia at the conditions found in a large two-stroke engine

combustion system. The simulation outcomes demonstrate excellent concordance with the experimental findings, accurately reflecting the main characteristics of combustion for both methanol and, notably, ammonia. The models' performance in capturing these processes enables a high degree of confidence in the related results.

Finally, the successful validation and calibration of the underlying models paved the way for creating a parametric 1-D model of the combustion system in an engine simulation environment with methanol/ammonia as the primary fuel source. The combined efforts of CFD investigations and experimental measurements gave a detailed insight into the combustion processes of both diesel and future fuels. These findings have important implications for understanding and modelling the combustion dynamics in large two-stroke marine engines which has been exemplarily demonstrated for the methanol combustion in this contribution.

In addition to the simulation toolbox development, the application of the presented approach resulted in identifying challenges of the methanol/ammonia injection and combustion process at an early stage of the technology development. For instance, the injection behaviour or the detection of possible locations of unburnt (e.g. NH_3 slip) or not completely burnt fuel such as N_2O, when referring to ammonia. Furthermore, this methodology is very cost-efficient and agile allowing for quick iterations between experiments and simulations.

The confidence gained from these numerical tools has allowed WinGD to apply the developed models to design combustion systems for the first production engines in their announced future fuel portfolio program.

Literature

[1] International Maritime Organization, "Resolution MEPC.377(80) – 2023 IMO Strategy on Reduction of GHG Emissions from Ships", 2023

[2] Global Maritime Forum, "The implications of the IMO Revised GHG Strategy for shipping", July 2023

[3] Schneiter, D., Goranov, S., Krähenbühl, P., Schäpper, D., Spahni, M., Weisser, G., "WinGD's X-act initiative: A holistic approach towards sustainable shipping", 18th Symposium "Sustainable Mobility, Transport and Power Generation", 2021

[4] Weisser, G., Goranov, S., Krähenbühl, P., Holtbecker, R., Zagorskiy, A., Schneiter, D., "Outlook on a decarbonised future of international shipping and how WinGD can contribute", 19th Symposium "Sustainable Mobility, Transport and Power Generation", 2023

[5] Hensel S., Gerber P., Karrer I., Schleppe Th., Schmidle M., Süess P., von Rotz B., Liu Bo: "Preparing for future demands – the CSSC Global 2-stroke Test Center", CIMAC 2023, Busan

[6] von Rotz B., Herrmann K., Weisser G., Cattin M., Bolla M. and Boulouchos K., "Impact of evaporation, swirl and fuel quality on the characteristics of sprays typical of large 2-stroke marine diesel engine combustion systems", ILASS-Europe, 2011.

[7] Herrmann K., Kyrtatos A., Schulz R. and Weisser G., von Rotz B., Schneider B. and Boulouchos B., "Validation and Initial Application of a Novel Spray Combustion Chamber Representative of Large Two-Stroke Diesel Engine Combustion Systems", ICLASS, 2009.

[8] Schmid A., von Rotz B., Bombach R., Weisser G., Herrmann K., and Boulouchos K., "Ignition Behaviour of Marine Diesel Sprays", COMODIA, 2012.

[9] von Rotz B., "Experimental Investigation of Spray Characteristics and Ignition Processes at Conditions representative of Large Two-Stroke Marine Diesel Engines", PhD thesis, No. 22968, ETH Zurich, 2015.

[10] von Rotz B., Herrmann K. and Boulouchos K., "Experimental Investigation on the Characteristics of Sprays Representative for Large 2-Stroke Marine Diesel Engine Combustion Systems", JSAE 20159074, 2015.

[11] Senecal P. K., "Multi-Dimensional Modeling of Direct-Injection Diesel Spray Liquid Length and Flame Lift-off Length using CFD and Parallel Detailed Chemistry", SAE, 2003-01-1043, 2003.

[12] Solomon, S., Qin D., Manning M., Chen Z., Marquis M., Averyt K.B., Tignor M., "Fourth Assessment Report of the Intergovernmental Panel on Climate Change", 2007, Cambridge University Press, Cambridge, United Kingdom and New York, NY, USA.